Arc Voltage Characteristics in Ultrahigh-Pressure Nitrogen Including Supercritical Region

Abid, F., Niayesh, K., Jonsson, E., Støa-Aanensen, N. S., & Runde, M.

Citation for the published version (APA 6th)
Abid, F., Niayesh, K., Jonsson, E., Støa-Aanensen, N. S., & Runde, M. (2017). Arc Voltage Characteristics in Ultrahigh-Pressure Nitrogen Including Supercritical Region. *IEEE Transactions on Plasma Science, PP*(99), 1-7. doi: 10.1109/TPS.2017.2778800

Arc Voltage Characteristics in Ultra-High Pressure Nitrogen Including Supercritical Region

Fahim Abid, Kaveh Niayesh, *Senior Member, IEEE*, Erik Jonsson, Nina Støa-Aanensen, and Magne Runde

***Abstract*—A supercritical fluid is formed when both pressure and temperature of a fluid exceed the critical point, where distinct gas and liquid phases no longer exist. Supercritical fluids demonstrate combined properties of gas and liquid, which make them interesting to investigate them as an arc extinction medium. This study focuses on the arc voltage characteristics of industrial grade nitrogen subjected to different filling pressures up to 98 bar including supercritical region. Pressure, arc duration, current and distance dependency of the arc are investigated by arc voltage measurement. It has been found that arc voltage increases with filling pressure without any abrupt change during the transition from gas into the supercritical region. Arc duration and current dependency of the arc voltage are not significant in the investigated parameter range. Arc voltage measurement with different electrode gaps suggests that the electrode voltage drop does not vary with filling pressure.**

***Index Terms*— Arc discharges, free-burning arc, supercritical fluid, switchgear, ultra-high pressure nitrogen.**

I. Introduction

An increasing number of windfarms located far off the coasts and also a growing demand for electric power supply to oil and gas installations on the seabed will lead to a development of an off-shore power transmission system. The substations (i.e., where all the components except the power cable are gathered) of such a system will be placed on the seabed and be remotely controlled instead of building expensive platforms or floaters. Placing the equipment on the seabed in many cases implies that it must be protected from the water pressure. For example, switching equipment such as circuit breakers need expensive solutions of encapsulations (to protect the equipment from high ambient pressure at seabed) and feedthroughs (to transfer power from the high-pressure water environment into the normal ambient pressure inside [1]). A novel concept based on filling the interrupting chamber with the same surrounding high pressure at seabed can substantially reduce the cost of the encapsulations and feedthroughs.

Air is a well known insulating material, where nitrogen is the main constituent. When the pressure and temperature exceed the critical pressure (P_c) and the critical temperature (T_c) as shown for nitrogen in Fig. 1 then it enters into a so-called supercritical (SC) region. Properties like the density, viscosity, diffusivity, thermal conductivity, and heat capacity of SC nitrogen lie in between the properties of the gaseous and the liquid phases of nitrogen [2]. For successful arc interruption, these properties are crucial, and hence, it is believed that SC nitrogen has the potential to be used as an interruption medium [3].

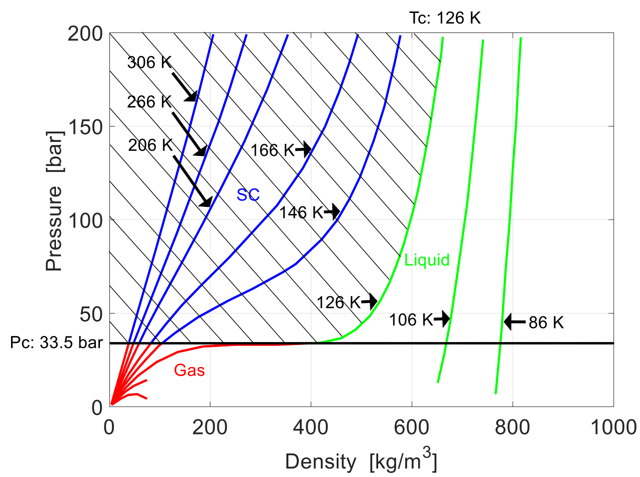

Fig. 1. Phase diagram of N_2, covering pressures up to 200 bar, temperatures in the range of 86–306K. P_c = 33.5 bar and T_c = 126 K [3]. The shaded part is the SC region.

Electric discharging inside a SC medium is a poorly studied phenomenon because of the unusually high pressures involved. Most of the previous works explore small-scale discharges of one millimeter or smaller inter-electrode gaps inside SC carbon dioxide [4]–[9] or SC nitrogen [2], [3], [10] under low energy dissipation, typically in the range of millijoules, while energy dissipations in switching arcs are normally up to hundreds of kilojoules. Exploring the arc properties in ultra-high pressure nitrogen including the SC region is a novel field of research. Arc experiments inside a high-pressure chamber can be hazardous without proper estimation of energy dissipation in the arc. As there is clearly a lack of experimental data of arc voltage in SC nitrogen, this work will help to estimate the energy dissipation in the arcing channel for further research of

Fahim Abid and Kaveh Niayesh are with the Department of Electrical Power Engineering, Norwegian University of Science and Technology (NTNU), Trondheim 7491, Norway (e-mail: fahim.abid@ntnu.no).

Nina Støa-Aanensen, Erik Jonsson and Magne Runde are with SINTEF Energy Research, Trondheim 7465, Norway.

switching arcs in SC nitrogen.

This paper explores the arcing voltage for arc burning between two identical fixed electrodes in nitrogen at different filling pressures. Nitrogen is chosen for its low critical temperature (126 K) and pressure (33.5 bar) as well as for its environmentally benign nature [11]. As the room temperature is well above the critical temperature of nitrogen, varying the pressure alone can facilitate the transition into the SC region. The arc duration and the current dependency of the arcing voltage are also investigated under different filling pressures. Finally, the electrode gap is varied to investigate the relation of the arc voltage and the arc length at different filling pressures.

II. Experimental Setup and Procedure

A. Test Circuit

The test circuit is shown in Fig. 2 and consists of a charging and a discharging section of a 4.8 µF high voltage (HV) capacitor, *C*. The capacitor can be charged to a predefined charging voltage of up to 20 kV through a diode resistor (D_c-R_c) unit. Once the capacitor is fully charged to the predefined level, switch S_1 can be opened to disconnect the charged capacitor from the grid.

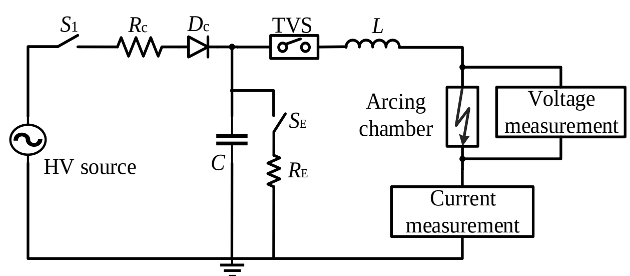

Fig. 2. Test circuit

The capacitor is discharged using a triggered vacuum switch (TVS) through the inductor, *L*, and further through an ignition copper wire inside the arcing chamber, see Fig. 2. An oscillation between the capacitor and the inductor generates a near sinusoidal current. The TVS allows only one-half cycle of the current to pass before it interrupts the current. Due to manual triggering of the TVS and the decay of the charged voltage through internal resistance of the capacitor, a ±5% error in the charging voltage is present. The 25 micron copper ignition wire melts due to adiabatic heating and subsequently creates the arcing channel. The capacitor is grounded using the earthing switch, S_E, once the test is over.

The arcing chamber is a 15.7 litres pressure tank rated for 500 bar and is shown schematically in Fig. 3. A 24 kV miniature HV cable is fed through the flange of the pressure tank (technique described elsewhere [12]) and held in position by several insulating supports. The ignition wire is fixed between two identical arc resistant copper-tungsten (CuW) electrodes of 10 mm diameter. The return path of the current is through the supporting metal structure and through the flange of the pressure tank. An HV probe is used for voltage measurement across the electrode gap and a current shunt is used to measure the current flowing through the arc. These data are sent via fiber optics connection to the control room where they are stored in a digital oscilloscope.

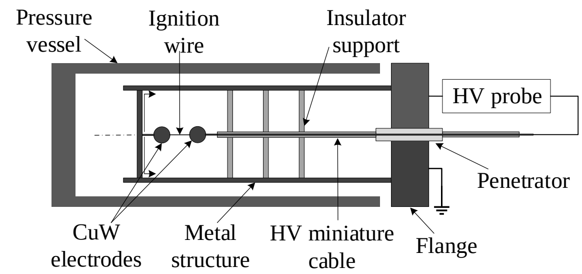

Fig. 3. Schematics of pressure vessel and the components inside.

B. Procedure

In the first and main experimental series the arc voltage has been investigated at different pressures, ranging from atmospheric up to 98 bar. The current amplitude was approximately 150 A, and the current pulse duration was about 1.43 ms for all tests. The contact distance has been kept constant at 20 mm.

To investigate the influence of arc duration on the arc voltage, a second series with different current pulse durations has been performed. Three different pulse durations were used; 0.59 ms, 1.43 ms, and 2.17 ms.

In the third series, the relationship between the arc voltage and the current amplitude has been studied. Tests at 150 A, 300 A, and 450 A were performed.

Finally, in the fourth series, the correlation between the electrode gap distance and arc voltage has been investigated. Experiments with gap distances from 5 mm to 30 mm have been carried out.

For the second, third and fourth series, experiments have been performed at four different pressure levels for each configuration; atmospheric pressure (1 bar), 15 bar, 30 bar, and 45 bar. All the test cases are summarized in Table I.

TABLE I
Test Cases and Conditions.

Test series	**Current amplitude [A]**	**Electrode gap distance [mm]**	**Current pulse duration [ms]**	**Nitrogen pressure [bar]**
1. Pressure dependency	150	20	1.43	1 to 98 (at 43 different levels)
2. Arc duration dependency	150	20	0.59, 1.43, 2.17	1, 15, 30, 45
3. Current dependency	150, 300, 450	20	0.59	1, 15, 30, 45
4. Distance dependency	150	5, 10, 15, 20, 25, 30	1.43	1, 15, 30, 45

Prior to each test, the pressure vessel is flushed with industrial grade nitrogen, ensuring that it contains 99% pure nitrogen for all the experiments conducted. After each experiment, the overpressure is released, the pressure vessel opened and a new arc ignition wire is mounted.

In addition to the main scope, the influence of metal vapor from the arc ignition wire is evaluated since this could be an error source to the above investigations. Tests with three different wire thicknesses are therefore performed.

III. Results

A typical measurement of the arc voltage and the arc current is shown in Fig. 4. First order Savitzky-Golay filtering is used to remove the inherent high frequency noise present in the measurement [13]. Filtering does not affect the results, as during the high current period of an alternating current, the arc voltage remains quite stable. Due to triggering of the TVS, a time delay of few tens of microseconds occurs between the trigger and the start of the conduction of current. This time delay is evident in the voltage measurement just after $t = 0$ ms. Due to joule heating, the voltage drop across the copper wire increases until voltage peaks just before 0.1 ms. The voltage peak corresponds to the evaporation of the copper wire and formation of arc channel. Once the arc is formed, the voltage drops quickly to a stable value. The arc voltage goes down slowly with time, showing free-burning arc characteristics.

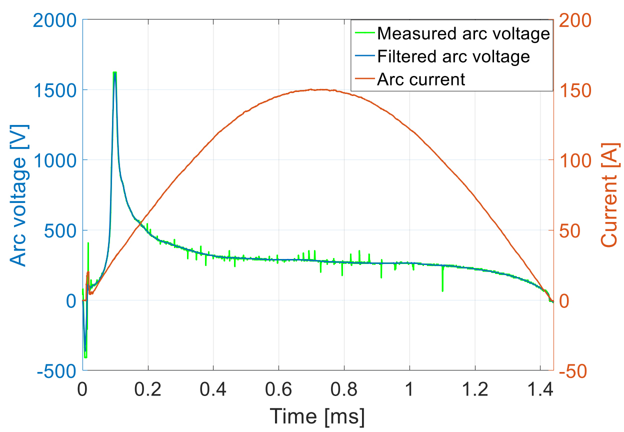

Fig. 4. Measured arc voltage and current at 45 bar filling pressures and 20 mm electrode gap.

A. Pressure Dependency

The main part of this work was to investigate the arc voltage as a function of filling pressure. In Fig. 5a, measured arc voltages with 20 bar interval of filling pressures are plotted. Clearly, the arc voltage increases with the filling pressure. The arc voltage even at high filling pressures, exhibits free-burning arc characteristics where the arc voltage goes down with time. High arc conductivity manifested as a decrease of the arc voltage before current zero indicates a very low interruption capability characteristic of free-burning arcs.

All the experiments from the pressure dependency investigations are plotted in Fig. 5b. Each point represents the arc voltage at current peak. The arc voltage increases from about 60-65 V at atmospheric pressure to approximately 450 V at 98 bar. The energy dissipation in the arc varied from 9 J to 68 J. The rate of increase of arc voltage with filling pressures is higher up to approximately 20 bar compared to after 20 bar. The gas enters into SC region at approximately 34 bar. Considering the stochastic nature of the arc and measurement uncertainty, no abrupt change in arc voltage near critical point is observed.

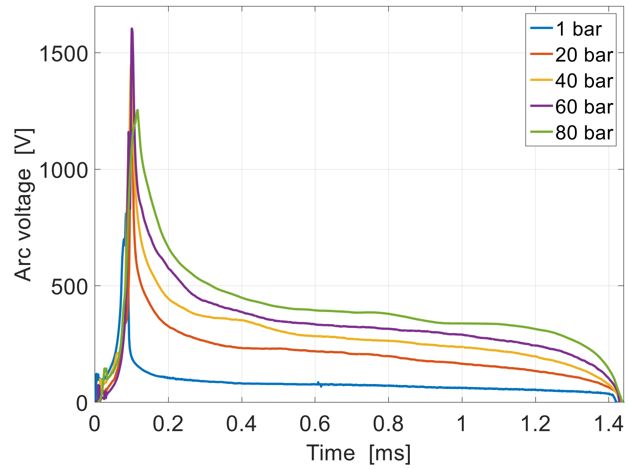

a) Measured arc voltage with 20 bar interval of filling pressures.

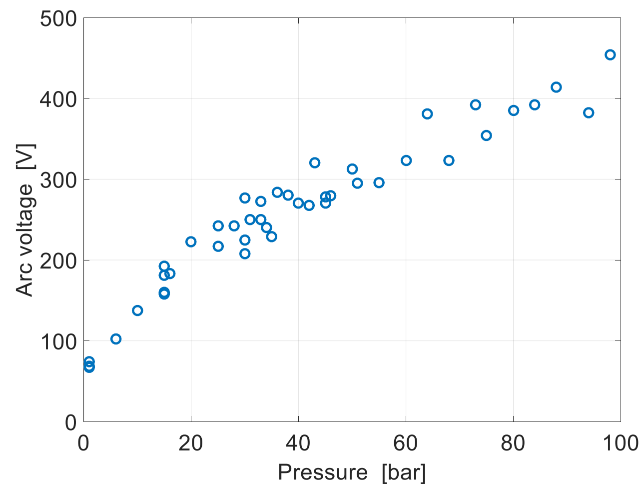

b) Arc voltage at current peak for different filling pressures.

Fig. 5. Arc voltage for arc current of 150 A, for half cycle current duration of 1.43 ms, at 20 mm electrode gap for different filling pressures.

B. Arc Duration Dependency

Fig. 6a shows the arc voltage versus the arc current for three different arc durations at atmospheric pressure. Oscillations after current zero due to stray capacitances are removed when plotted in Fig. 6a, as the focus of this study is on the arcing period and not on the period after current zero. The arc initiation time corresponding to the voltage peak varies with current duration, which is expected due to the high rate of change of current at shorter current durations. The arc voltage at the current peak as a function of the current duration for different filling pressures is plotted in Fig. 6b. For the current durations of 0.59 ms, two measurements for each case have been performed and the average is plotted with the error bar. Due to the complexity of the test and long time required for preparation of each experiment, no statistical data is gathered further in this paper. Nevertheless, for pressure dependency measurements shown in Fig. 5b, same tests were repeated for some cases (e.g., at 1 bar, 15 bar, 30 bar etc.), which can provide an estimation of measurement variations. Based on the results shown in Fig. 6b, no strong arc duration dependency is observed from the measurement.

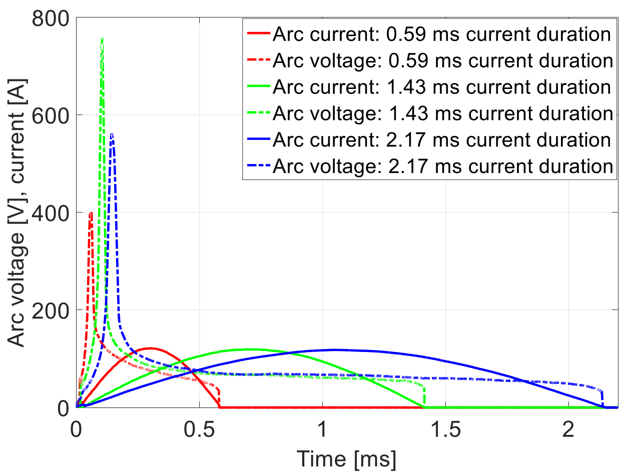

a) Measured arc voltage and current at atmospheric pressure with different current durations.

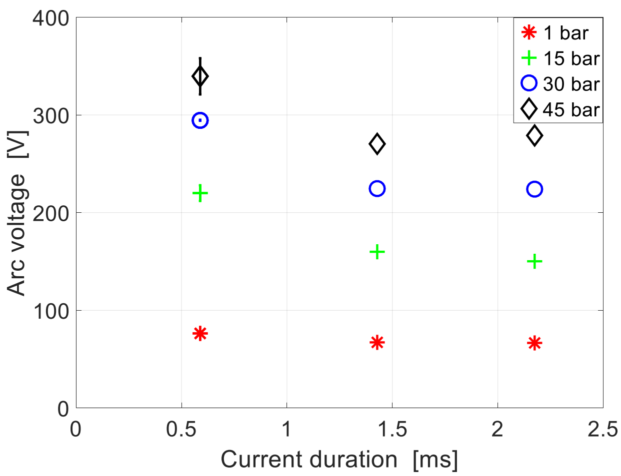

b) Arc voltage at the current peak for different current durations at different filling pressures.

Fig. 6. Arc voltage as a function of the current duration for arc current of 150 A, at 20 mm electrode gap.

C. *Current Dependency*

The arc voltage as a function of the arc current is illustrated in Fig. 7. The arc voltages for 20 mm electrode gap at atmospheric pressure for three different current levels are found to be 78 V, 80 V, and 87 V, respectively. For a higher filling pressure of 45 bar, arc voltages for three different current levels are 358 V, 303 V, and 302 V, respectively. No significant current dependency is apparent in the investigated range.

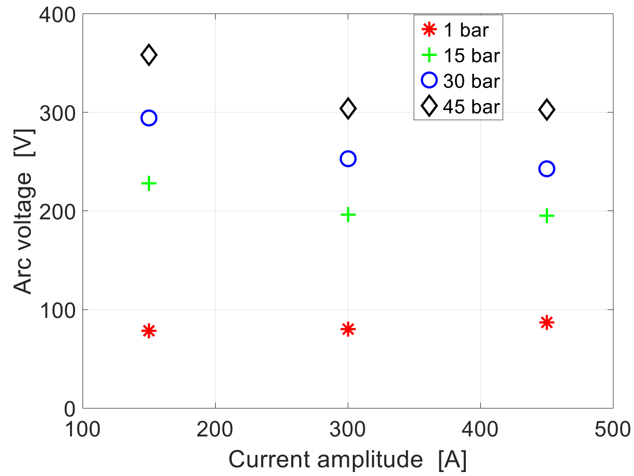

Fig. 7. Current dependency of arc voltage for 20 mm electrode gap for current duration of 0.59 ms.

D. *Distance Dependency*

The correlation between the electrode gap and the arc voltage is explored by changing the electrode gap from 5 mm to 30 mm with 5 mm increments and is shown in Fig. 8. Considering a linear relationship between the arc voltage and the electrode gap, if the data is extrapolated to 0 mm arcing distance, the electrode voltage drop otherwise known as cathode and anode fall of potential can be estimated. This electrode drop is found to be approximately 33-37 V for the tested filling pressures. It is high compared to the typical electrode voltage drop of around 16 V for 26 mm diameter CuW electrode for arc at atmospheric pressure in air [14]. Such large deviation in electrode voltage drop is probably due to presence of non-linear characteristics of arc voltage with arc lengths below 5 mm. For 5 mm and larger electrode gaps, the experimental results are in line with the literature [14].

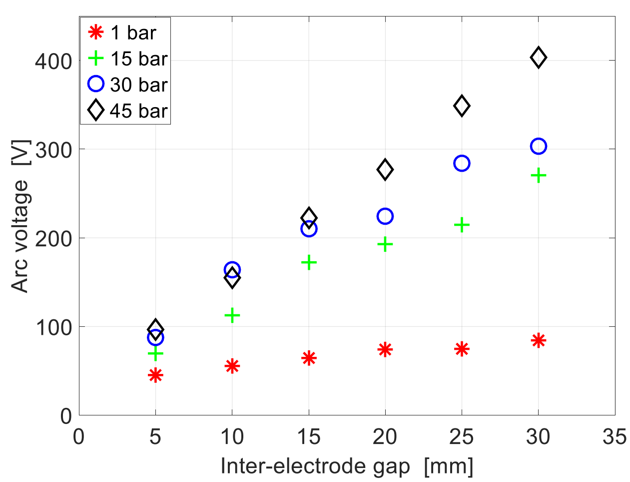

Fig. 8. Distance dependency of arc voltage for 150 A current for 1.43 ms current duration for different filling pressures.

E. *Effect of Metal Vapor*

To investigate the effect of metal vapor in the measured data, ignition wires of different thicknesses are used and the results are plotted in Fig. 9. It is assumed that the energy dissipated in the ignition wire is responsible for temperature increase and melting and evaporation of the wire. Time and voltage peak corresponding to ignition wire evaporation are estimated using the temperature dependent resistivity and specific heat of copper from literature [15]–[18]. The estimation of voltage peak corresponding to ignition fits well with the experimental results. The presence of metal vapor generally leads to a reduction in the arc temperature due to an increase in the radiative emission. The increased electrical conductivity due to metal vapor tends to reduce the arc voltage, however the temperature decrease associated with strong radiative emission has the opposite effect due to temperature dependent conductivity. This may explain the increase of arc voltage observed for 100 micron ignition wire [19]. Considering the arc voltage measured for 25 and 40 micron ignition wires, it can be concluded that metal vapor in the above experiments does not have any significant effect on the arc voltage.

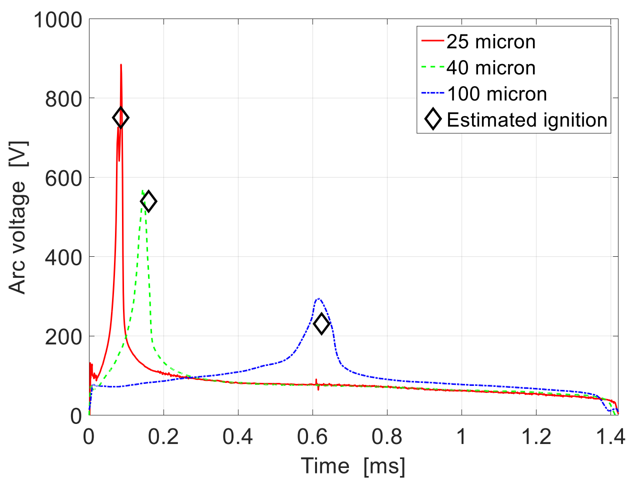

Fig. 9. Measured and estimated ignition time with different thickness of ignition wire at atmospheric pressure for arc current of 150 A at 20 mm electrode gap.

IV. Discussions

The increase of the arc voltage with filling pressure is obvious from the results. Low currents (i.e., less than 30 A) and high currents (i.e., more than 30A) arc properties differ significantly from each other due to different physical processes dominating in the arc [20]. In this paper, all of the experiments were conducted at current amplitude of 150 A or higher, which lie in the high current region. Primarily, the arc temperature at the arc center can be determined by the energy balance equation:

$$\frac{I^2}{\sigma A^2} = \frac{4\pi kT}{A} + U, \quad (1)$$

where I is the arc current, σ is the electrical conductivity, A is the arc cross section area, T is the temperature of the arc, k is the thermal conductivity, and U is the net radiation emission coefficient. For low current arcs, due to the low temperature in the arc, the radiation is negligible and natural convection is the dominant cooling process. High current arc properties are mainly determined by magnetically induced convection. The magnetic flux density, B, of the arc produces a compressive force inwards on the arc:

$$(J \times B)_r = -\frac{\mu\sigma E^2}{r}\int_0^r x\sigma dx, \quad (2)$$

where J is the current density, E is the electric field and $\mu = 1.26\times10^{-8}$ Hcm^{-1}. This compressive force is balanced by an increase in the pressure inside the arc:

$$\Delta P = \frac{\mu I^2}{4\pi A}\left(1-\frac{r^2}{R^2}\right), \quad (3)$$

where r the radial position, and R is the radius of the isothermal plasma. According to (3), a smaller arc cross section results in a higher pressure near the electrodes where the current density is the highest. A strong convective flow is induced by this axial pressure gradient. The radiation emission coefficient increases rapidly with the temperature, so that for high currents, the term U dominates the conduction term in (1). Based on many assumptions (described elsewhere [20]), Lowke estimated the electric field of the high current arc:

$$E = \frac{I}{\sigma A} = 0.26\left(\frac{h}{\sigma z}\right)^{0.5}(\mu J_0 \rho)^{0.25} I^{0.25} \quad (4)$$

where h is the enthalpy of the plasma, ρ is the density, J_0 is the current density at the cathode, and z is the axial distance from the cathode. It can be seen from (4) that the electric field is related to the density of the medium. This explains the high arcing voltage at higher filling pressures.

The arc contracts with increasing filling pressure which results in high current densities and in high electric fields [21]. The radiation coefficient also increases with the filling pressure, resulting in a better cooling at higher filling pressures. Hence, the temperature in the arc core decreases with filling pressure [20]. Reduction of arc temperature decreases the conductivity of arc channel, which increases the voltage drop over the arc. From the simple theory of free-burning arcs given by Lowke [20], the estimated electric field for 10 kA and 10 A arc current from theory and the calculated electric field from the measurements in this paper are plotted in Fig. 10. Here, the electric field is assumed homogeneous in the arc column and is calculated by subtracting the electrode voltage drop.

The arc voltage of pressurized air up to 9 bar has been reported in literature where researchers also found an increasing arc voltage with increasing filling pressure [22]. No strong current dependency was reported for currents below 1 kA, and the electrode voltage drop was in the range of 30 to 40 V [22]. These findings are in agreement with our measurements. Arc voltages in the range of approximately 100 V have been reported for an electrode gap of 1.8 mm at 50 bar filling pressure of nitrogen, which is higher than our observation [23].

However, the experiments were conducted at frequencies of more than 3 kHz and with currents up to few tens of amperes. Lower currents, higher frequency, and different electrode size, all can have an influence on the arc voltage.

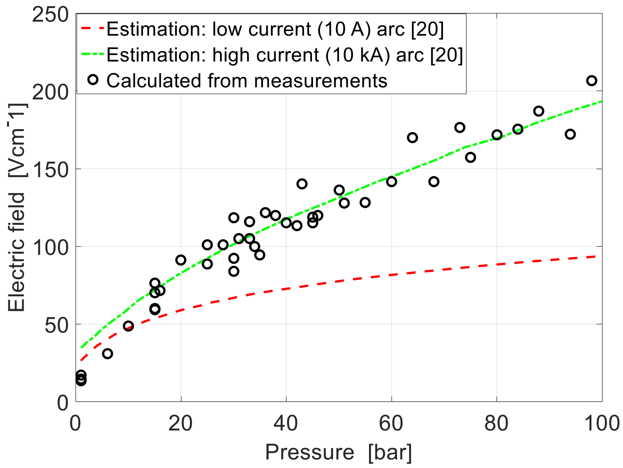

Fig. 10. Estimations from Lowke [20] and calculated electrical field from measured arc voltage with different filling pressures (arc current: 150 A, current duration: 1.43 ms).

The density variation is not abrupt at room temperature when transition to SC happens, as shown in Fig. 1. Researchers found that breakdown field strength of synthetic air, carbon dioxide (CO_2), a mixture of CO_2 and oxygen (O_2), and tetrafluoromethane (CF_4) shows a saturation of the breakdown electric field strength above 20 bar [24]. It was also concluded that, if the gas becomes supercritical, there is no change in the breakdown electric field strength. Although the arc voltage and the breakdown voltage are not directly correlated, both observations are in line.

V. Conclusions

The arc voltage in 99% pure nitrogen at different filling pressures (from atmospheric pressure up to 98 bar) including the supercritical region has been investigated for medium voltage ratings and currents in the range of 150 to 450 A. Based on the experimental findings, the following conclusions have been drawn:

- The arc voltage increases with increasing filling pressure.
- The arc voltage does not change abruptly when the transition from gas to supercritical region occurs.
- The arc duration dependency of the arc voltage is not significant for current durations of 0.59 ms up to 2.17 ms for filling pressures up to 45 bar.
- The current dependency of the arc voltage is not significant for currents of 150 A to 450 A and filling pressures up to 45 bar.

References

[1] T. Hazel, H. H. Baerd, J. J. Legeay, and J. J. Bremnes, “Taking power distribution under the sea: design, manufacture, and assembly of a subsea electrical distribution system,” *IEEE Ind. Appl. Mag.*, vol. 19, no. 5, pp. 58–67, Sep. 2013.

[2] J. Zhang *et al.*, “Breakdown strength and dielectric recovery in a high pressure supercritical nitrogen switch,” *IEEE Trans. Dielectr. Electr. Insul.*, vol. 22, no. 4, pp. 1823–1832, Aug. 2015.

[3] J. Zhang, A. H. Markosyan, M. Seeger, E. M. van Veldhuizen, E. J. M. van Heesch, and U. Ebert, “Numerical and experimental investigation of dielectric recovery in supercritical N_2,” *Plasma Sources Sci. Technol.*, vol. 24, no. 2, p. 25008, Feb. 2015.

[4] M. Goto *et al.*, “Reaction in plasma generated in supercritical carbon dioxide,” *J. Phys. Conf. Ser.*, vol. 121, no. 8, p. 82009, Jul. 2008.

[5] T. Ito and K. Terashima, “Generation of micrometer-scale discharge in a supercritical fluid environment,” *Appl. Phys. Lett.*, vol. 80, no. 16, pp. 2854–2856, Apr. 2002.

[6] E. H. Lock, A. V. Saveliev, and L. A. Kennedy, “Influence of electrode characteristics on dc point-to-plane breakdown in high-pressure gaseous and supercritical carbon dioxide,” *IEEE Trans. Plasma Sci.*, vol. 37, no. 6, pp. 1078–1083, Jun. 2009.

[7] H. Tanoue *et al.*, “Shock wave generated by negative pulsed discharge in supercritical carbon dioxide,” in *2013 19th IEEE Pulsed Power Conference (PPC)*, 2013, pp. 1–5.

[8] Z. B. Yang, S. H. R. Hosseini, T. Kiyan, S. Gnapowski, and H. Akiyama, “Post-breakdown dielectric recovery characteristics of high-pressure liquid CO_2 including supercritical phase,” *IEEE Trans. Dielectr. Electr. Insul.*, vol. 21, no. 3, pp. 1089–1094, Jun. 2014.

[9] H. Tanoue, T. Furusato, K. Takahashi, S. H. R. Hosseini, S. Katsuki, and H. Akiyama, “Characteristics of shock waves generated by a negative pulsed discharge in supercritical carbon dioxide,” *IEEE Trans. Plasma Sci.*, vol. 42, no. 10, pp. 3258–3263, Oct. 2014.

[10] J. Zhang, B. van Heesch, F. Beckers, T. Huiskamp, and G. Pemen, “Breakdown voltage and recovery rate estimation of a supercritical nitrogen plasma switch,” *IEEE Trans. Plasma Sci.*, vol. 42, no. 2, pp. 376–383, Feb. 2014.

[11] J. V Sengers and J. M. H. L. Sengers, “Thermodynamic behavior of fluids near the critical point,” *Annu. Rev. Phys. Chem.*, vol. 37, no. 1, pp. 189–222, Oct. 1986.

[12] J. Aakervik, G. Berg, and S. Hvidsten, “Design of a high voltage penetrator for high pressure and temperature laboratory testing,” in *2011 Annual Report Conference on Electrical Insulation and Dielectric Phenomena*, 2011, pp. 267–270.

[13] R. W. Schafer, "What is a savitzky-golay filter? [lecture notes]," in IEEE Signal Processing Magazine, vol. 28, no. 4, pp. 111-117, July 2011.

[14] Y. Yokomizu, T. Matsumura, R. Henmi, and Y. Kito, “Total voltage drops in electrode fall regions of SF_6 , argon and air arcs in current range from 10 to 20 000 a,” *J. Phys. D. Appl. Phys.*, vol. 29, no. 5, pp. 1260–1267, 1996.

[15] E. M. Apfel’baum, “Calculation of the electrical conductivity of liquid aluminum, copper, and molybdenum,” *High Temp. from Teplofiz. Vysok. Temp.*, vol. 41, no. 4, pp. 466–471, 2003.

[16] J. Brillo and I. Egry, “Density determination of liquid copper, nickel, and their alloys,” *Int. J. Thermophys.*, vol. 24, no. 4, pp. 1155–1170, 2003.

[17] G. Lohöfer, “Electrical resistivity measurement of liquid metals,” *Meas. Sci. Technol.*, vol. 16, no. 2, pp. 417–425, Feb. 2005.

[18] V. Y. Chekhovskoi, V. D. Tarasov, and Y. V. Gusev, “Calorific properties of liquid copper,” *High Temp. Transl. from Teplofiz. Vysok. Temp.*, vol. 38, no. 3, pp. 394–399, May 2000.

[19] J. Haidar, “The dynamic effects of metal vapour in gas metal arc welding,” *J. Phys. D. Appl. Phys.*, vol. 43, no. 16, p. 165204, Apr. 2010.

[20] J. J. Lowke, “Simple theory of free-burning arcs,” *J. Phys. D. Appl. Phys.*, vol. 12, no. 11, pp. 1873–1886, Nov. 1979.

[21] K. C. Hsu and E. Pfender, “Modeling of a free-burning, high-intensity arc at elevated pressures,” *Plasma Chem. Plasma Process.*, vol. 4, no. 3, pp. 219–234, Sep. 1984.

[22] S. Watanabe, K. Kokura, K. Minoda, and S. Sato, “Characteristics of the arc voltage of a high-current air arc in a sealed chamber,” *Electr. Eng. Japan*, vol. 186, no. 1, pp. 34–42, Jan. 2014.

[23] J. Zhang, “Supercritical fluids for high power switching,” Technische Universiteit Eindhoven, 2015.

[24] M. Seeger, P. Stoller, and A. Garyfallos, “Breakdown fields in synthetic air, CO_2, a CO_2/ O_2 mixture, and CF_4 in the pressure range 0.5–10 mpa,” *IEEE Trans. Dielectr. Electr. Insul.*, vol. 24, no. 3, pp. 1582–1591, Jun. 2017.

Fahim Abid received the B.Sc. degree in electrical and electronic engineering from the Islamic University of Technology (IUT), Dhaka, Bangladesh in 2012. He received the M.Sc. degree in electrical engineering combinedly from Royal Institute of Technology (KTH), Stockholm, Sweden and Technical University Eindhoven (TU/e), Eindhoven, Netherlands in 2015. He is currently working as a PhD candidate at the department of electric power engineering in Norwegian University of Science and Technology (NTNU), Trondheim, Norway.

Kaveh Niayesh (S'98–M'01–SM'08) received the B.Sc. and M.Sc. degrees in electrical engineering from the University of Tehran, Tehran, Iran, in 1993 and 1996, respectively, and the Ph.D. degree in electrical engineering from the RWTH-Aachen University of Technology, Aachen, Germany, in 2001. During the last 16 years, he held different academic and industrial positions including Principal Scientist with the ABB Corporate Research Center, Baden-Dattwil, Switzerland; Associate Professor with the University of Tehran; and Manager, Basic Research, with AREVA T&D, Regensburg, Germany. Currently, he is a Professor with the Department of Electric Power Engineering, Norwegian University of Science and Technology (NTNU). He is the holder of 16 patents and has more than 95 journal and conference publications on current interruption and limitation, vacuum and gaseous discharges, plasma modeling and diagnostics, switching transients, and pulsed power technology.

Erik Jonsson received the M.Sc. degree in physics from Uppsala University, Uppsala, Sweden, in 2005 and the Ph.D. degree in electrical power engineering at Norwegian University of Science and Technology (NTNU), Trondheim, Norway, in 2014. From 2006 to 2007, he was with ABB Corporate Research, Västerås, Sweden. Currently, he is with SINTEF Energy Research, Trondheim, Norway, working with medium-voltage switchgear and power cables.

Nina Sasaki Støa-Aanensen received the M.Sc. degree in applied physics and mathematics and the Ph.D. degree in electrical power engineering from the Norwegian University of Science and Technology (NTNU), Trondheim, Norway, in 2011 and 2015, respectively. She is currently working with SINTEF Energy Research, Trondheim, Norway.

Magne Runde received the M.Sc. degree in physics and the Ph.D. degree in electrical power engineering from the Norwegian University of Science and Technology (NTNU), Trondheim, Norway, in 1984 and 1987, respectively. He has been with SINTEF Energy Research, Trondheim, since 1988. From 1996 to 2013, he was an Adjunct Professor of High Voltage Technology, NTNU. His fields of interest include circuit breakers and switchgear, electrical contacts, power cables, diagnostic testing of power apparatus, and power applications of superconductors. Dr. Runde has been the convener and member of several CIGRÉ working groups; authored and co-authored more than 45 articles in peer-reviewed international journals and more than 60 conference publications.